4-15-1996

# Explosive compaction of Magnequench Nd–Fe–B magnetic powders

S. Guruswamy
*University of Utah, Salt Lake City, Utah*

M.K. McCarter
*University of Utah, Salt Lake City, Utah*

Jeffrey E. Shield
*University of Nebraska - Lincoln*, jshield@unl.edu

V. Panthanachan
*Magnequench, Delphi(E), General Motors Corp., Anderson, Indiana*

# Explosive compaction of Magnequench Nd–Fe–B magnetic powders

S. Guruswamy, M. K. McCarter, and J. E. Shield
*University of Utah, Salt Lake City, Utah 84112*

V. Panchanathan
*Magnequench, Delphi(E), General Motors Corp., Anderson, Indiana 46013*

Magnequench NdFeB powders having high and low rare earth contents were explosively compacted to obtain cylindrical magnets. The magnetic properties were found to be isotropic and were superior to conventionally consolidated isotropic magnets. The $(BH)_{max}$ was 14.7 MGOe and the remanence was 8.7 kG for the explosively compacted magnet with lower rare earth content. X-ray diffraction patterns confirm the explosively compacted magnet to be crystalline and the predominant phase to be the 2-14-1 phase. Transmission electron microscopy examination showed a microstructure to consist of 20–25 nm size equiaxed grains consistent with the magnetic measurements. © *1996 American Institute of Physics.* [S0021-8979(96)38408-5]

## I. INTRODUCTION

High $(BH)_{max}$, use of less strategic Nd, and high concentration of low cost Fe and B have made NdFeB alloys extremely attractive for many high-performance permanent magnet applications.[1–5] With higher $(BH)_{max}$, high power levels and high magnetic fields can be obtained using smaller magnets and consequently the use of NdFeB magnets, with $(BH)_{max}$ in the range of 35–40 MGOe, has resulted in revolutionary developments in the miniaturization of motors, actuators and sensors, and other devices critical to a wide range of industries and technologies.

The Magnequench division of General Motors produces NdFeB magnetic powders by melt spinning ribbons of NdFeB alloy followed by comminution. These powders are used to make polymer bonded magnets, hot pressed isotropic magnets, and hot deformed anisotropic magnets.[1–4] The microstructure developed by these processes consists of grains of the hard magnetic phase $Nd_2Fe_{14}B$ separated by a nonmagnetic grain boundary phase.[1,5–7]

Powders can also be consolidated with shock waves in the appropriate pressure range and duration for a given powder.[8–12] The shock waves may be generated by detonating shaped explosive charge in contact with the powder container or by impact with a high velocity projectile. The pressures in the shock front that moves through the powder are several times the flow stress of the material, typically several GPa. Consolidation occurs by particle deformation followed by extrusion in to the void space. The material near the surface of the particle will see temperature pulses exceeding the melting point over durations that range from microseconds to milliseconds but quickly quenched by heat flow in to the bulk of the powder particle. Thus it is possible to nearly preserve the original microstructures that have been obtained by the rapid solidification processing of the powder. Densities approaching theoretical density can be achieved by a proper choice of pressure and pulse duration. Also effective breakup of adherent oxide film can be achieved minimizing the tendency to fracture along prior particle boundaries.

University of Utah in collaboration with Magnequech is carrying out explosive compaction studies of isotropic and anisotropic powders to obtain full density. This article examines the influence of explosive compaction on the magnetic properties and microstructures of two isotropic NdFeB powders. The two powders, one containing lower amount of rare earth and the other containing an higher amount of rare earth, are examined. The explosively compacted magnets were characterized using x-ray diffraction, scanning electron microscopy and transmission electron microscopy. The magnetic properties were examined with a vibrating sample magnetometer.

## II. EXPERIMENTAL WORK

Two isotropic powders used in this study were MQP-A powder and MQP-B powder. The nominal composition of the MQP-A powder was Fe-30.5 wt % total rare-earth-0.9 wt % B and that of powder MQP-B was Fe-5 wt % Co-27.5 wt % total rare-earth-0.9 wt % B. The rare earth component consisted of mainly Nd with 0.5% (max) of Pr and 0.2 wt % (max) of other rare earths. The powders were packed in a copper tube closed at one end with a tight-fitting steel rod. The open end of copper tube was then sealed with a steel cap. The packed density of the powder was ~55%. The cop-

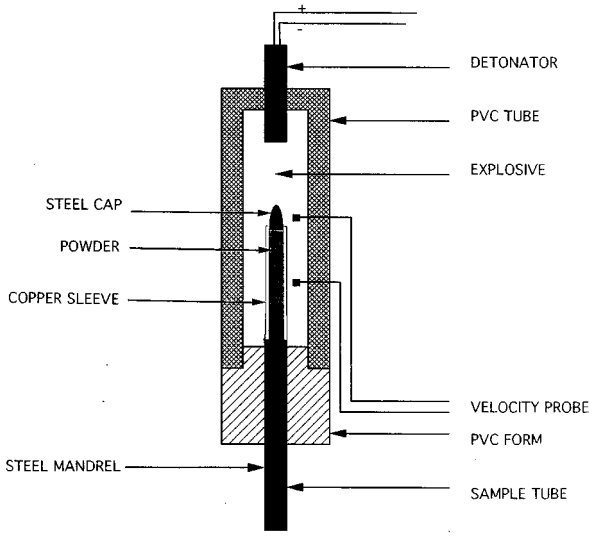


FIG. 1. Explosive container assembly for explosive compaction of NdFeB powders.

 0021-8979/96/79(8)/4851/3/$10.00  

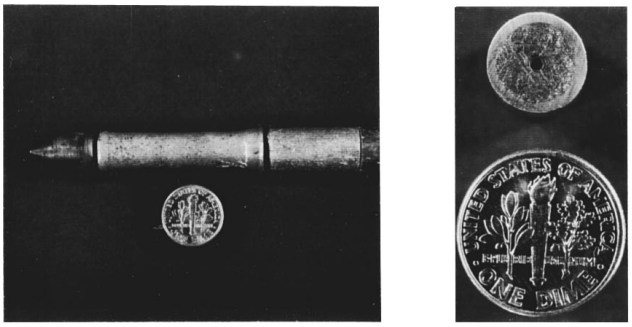


FIG. 2. (a) An explosively compacted NdFeB magnet and (b) micrograph of a cross section of the FeNdB magnet piece shown in (a).

per tube assembly containing the powder was placed centrally in an explosive charge container as shown in Fig. 1. The cylindrical detonator fuse was inserted in the snugly fitting hole in the cap of the PVC container. The liquid-slurry explosive Dyno Nobel 207X was prepared by mixing the two components, perchlorate-base liquid component A and an aluminum-based component B. The mixture was then poured into the container, which was closed with the cap assembly containing the compacted copper tube. The weight of the explosive charge used for the compaction experiments was ~350 g.

Explosive compaction using large amounts of explosive charges as indicated above were performed at the Dyno Nobel facilities just outside of Salt Lake City. The shock wave velocity was measured in several explosive experiments using two triggers placed at different locations of the container. Typical shock wave velocities achieved in these experiments were ~4300 m/s. The detonation velocity is related to the compaction pressure by the following relation,[13]

$$\mathrm{DP}=2.325\times10^{-7}\rho(\mathrm{VOD})^2,$$

where VOD is the velocity of detonation in ft/s, DP is the detonation pressure in kbar, and $\rho$ is the density of the explosive mix in g/cc. The resulting compaction pressure was ~6 GPa. The explosively compacted specimens prepared from MQP-A powder and MQP-B powder are hereafter referred to as EC-A and EC-B, respectively.

Optical microscopy and scanning electron microscopy techniques were used to examine the porosity and crack size distribution in EC-A and EC-B specimens. The microstructure was examined by transmission electron microscopy (TEM) using a Jeol 2000 FX II STEM. X-ray diffraction was performed using a Siemens D5000 diffractometer. Differential thermal analysis was carried out using a Perkin Elmer $\mathrm{DTA}^{-7}$ system. Specimens 4.5 mm×4.5 mm×4.5 mm in size were used for the magnetic measurements using a vibrating-sample magnetometer (VSM).

## III. RESULTS AND DISCUSSION

Figure 2(a) shows an optical micrograph of one of the explosively compacted piece and Fig. 2(b) shows a cross section of the compacted piece. The sample shows in general excellent compaction with some cracking. A central hole is

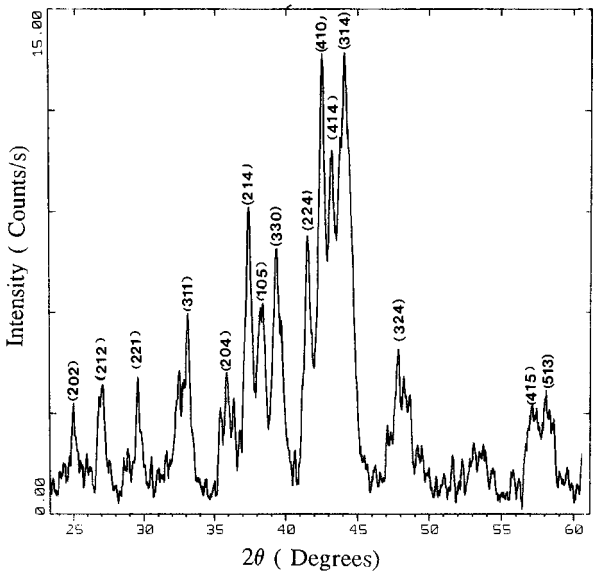


FIG. 3. X-ray diffraction pattern of explosively compacted EC-B magnet.

observed along the axis of the cylindrical piece and this arises from the melting and ejection of material under the focussed energy of the shock waves near the center. The hole is called the Mach stem and results from an excessive consolidation pressure.[9] The size of the hole was observed to decrease in the direction of shock wave propagation and was not observed in over a 5 mm length at the other end. This hole can be eliminated by lowering the detonation pressure or by having an additional copper tube sleeve surrounding the tube that contains the powder.[10,14] The cracks observed arise from the tensile component of the reflected shock waves. These can be minimized or eliminated by controlling the ratio of the explosive charge to the powder, the detonation pressure and the use of a two tube design as mentioned earlier. No significant variation in the porosity distribution

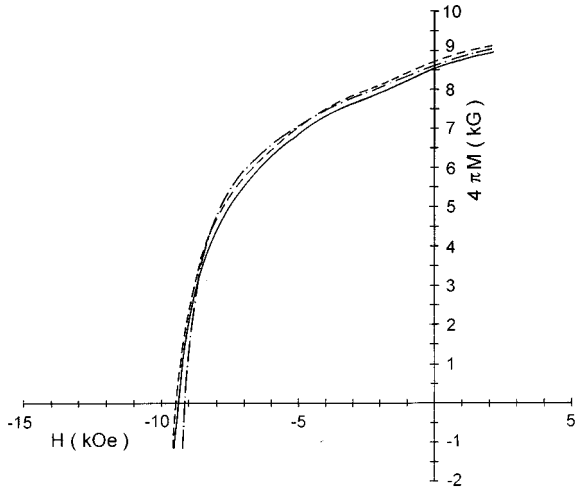


FIG. 4. Demagnetization curves for three orthogonal directions in EC-B magnet.

TABLE I. Magnetic properties of EC-A and EC-B magnet.

| Specimen orientation | $M_s$ (kG) | $B_r$ (kG) | $H_{ci}$ (kOe) | $BH_{max}$ (MGOe) |
|---|---|---|---|---|
| | EC-A magnet | | | |
| $z$-direction | 8.6 | 7.63 | 14.57 | 11.41 |
| $x$-direction | 7.94 | 7.51 | 14.51 | 11.03 |
| $y$-direction | 8.00 | 7.59 | 14.46 | 11.53 |
| | EC-B magnet | | | |
| $z$-direction | 8.96 | 8.54 | 9.41 | 14.05 |
| $x$-direction | 9.11 | 8.72 | 9.47 | 14.72 |
| $y$-direction | 9.02 | 8.64 | 9.17 | 14.58 |

and cracking was observed along the length of the compact. The density of specimen EC-A was 7.2 g/cc while the density of EC-B was 7.3 g/cc.

Figure 3 shows an x-ray diffraction pattern obtained for explosively compacted MQP-B powder. The peaks observed correspond to 2-14-1 phase. This confirms that the material is still crystalline and contains predominantly the hard 2-14-1 phase. The amount of other possible phases was small and could not be identified from this pattern. The differential thermal analysis of the compacts revealed a major peak at 1172 °C, corresponding to the melting of the 2-14-1 phase.

Demagnetization curves determined using a VSM in three orthogonal directions showed that the magnetic properties were isotropic in both EC-A and EC-B magnets. Figure 4 shows the demagnetization curves for EC-B magnet. Table I summarizes the values of $B_r$, $H_{ci}$, and $BH_{max}$ for the two specimens obtained from the demagnetization curve which shows essentially no difference in magnetic properties measured along the three orthogonal directions. This is expected as the explosive compaction occurs under nearly isostatic compressive pressure conditions and the microstructure of the ribbons are nearly preserved. In Table II, the magnetic properties of bonded isotropic magnets, and hot pressed magnets are compared with the explosively compacted magnets. The $BH_{max}$ values observed are higher and comparable to hot pressed magnets.[3,4] The densities observed in the present EC-A and EC-B specimens are ~95%. The explosive compaction could achieve nearly 100% density

TABLE II. Comparison of magnetic properties of EC-A and EC-B magnets with bonded and hot pressed magnets.[3,4]

| Sample | $B_r$ (kG) | $H_{ci}$ (kOe) | $BH_{max}$ (MGOe) |
|---|---|---|---|
| EC-A magnet | 7.6 | 14.5 | 11.3 |
| EC-B magnet | 8.6 | 9.4 | 14.5 |
| MQ1-A isotropic magnet | 6.3 | 15.0 | 9.0 |
| MQ1-B isotropic magnet | 6.9 | 9.0 | 10.0 |
| MQ2 isotropic hot pressed magnet | 8.0 | 18.0 | 14.0 |

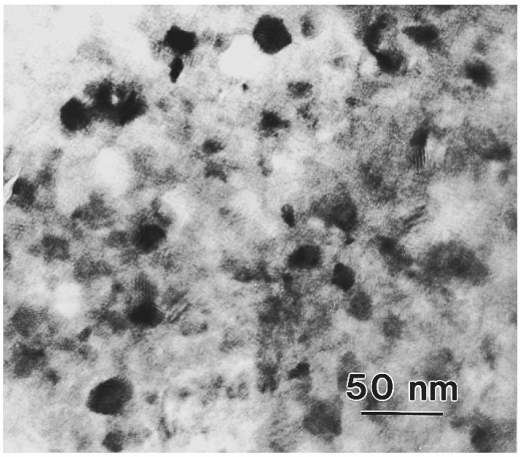


FIG. 5. A TEM micrograph of an EC-B specimen.

and hence a >10% increase in $BH_{max}$ is possible by this processing route which makes this approach very attractive.

Figure 5 shows a TEM image of an EC-B specimen. The microstructure consists of equiaxed grains on the order of 20–25 nm. This microstructure is similar to that observed in the original ribbon. The equiaxed microstructure observed is consistent with the isotropic properties observed for specimens EC-A and EC-B. It is very important to note that the explosive compaction has preserved the rapidly solidified ribbon microstructure and therefore do not have any adverse effects of grain growth. Further TEM work is in progress to understand the enhancement in magnetic properties by explosive compaction.

## ACKNOWLEDGMENTS

The support of this work by GM–Magnequench and Dyno Nobel through the provision of materials, experimental facilities, and personnel for the explosive compaction experiments is gratefully acknowledged.

[1] J. J. Croat and J. F. Herbst, Mater. Res. Soc. Bull. **XIII**, 37 (1988).
[2] J. F. Herbst, Rev. Mod. Phys. **63**, 819 (1991).
[3] V. Panchanathan, J. Mater. Eng. **11**, 51 (1989).
[4] J. J. Croat, IEEE Trans. Magn. **MAG-25**, 3550 (1989).
[5] M. Sagawa, S. Hirosawa, H. Yamamotto, S. Fujimura, and Y. Matsuura, Powder Metall. **35**, 785 (1992).
[6] R. K. Mishra, Mater. Sci. Eng. B **7**, 297 (1991).
[7] A. Hutten, J. Met. **44**, 11 (1992).
[8] R. N. Wright, G. E. Korth, and J. E. Flinn, Adv. Mater. Proc. **132**, 56 (1987).
[9] L. E. Murr and K. P. Staudhammer, in *Shock Waves For Industrial Applications*, edited by L. E. Murr (Noyes, Park Ridge, NJ, 1988), pp. 1–57.
[10] M. A. Meyers, N. N. Tadhani, and L. H. Yu, in Ref. 9, pp. 265–334.
[11] *Metals Handbook*, 10th ed. (ASM, Metals Park, OH, 1984), Vol. 7, pp. 305 and 692.
[12] R. Prummer, in *Explosive Welding, Forming and Compaction*, edited by T. Z. Blazynski (Applied Science, New York, 1983), pp. 369–389.
[13] *Explosives and Rock Blasting* (Atlas Powder Company, Dallas, TX, 1987), p. 18.
[14] A. Ferreira and M. A. Meyers, in *Shock-Wave and High-Strain Rate Phenomena in Materials*, edited by M. A. Meyers, L. E. Murr, and K. P. Staudhammer (Marcel Dekker, New York, 1992), pp. 361–370.